ARCHIVES OF METALLURGY

Volume 47 2002 Issue 3

WIKTORIA RATUSZEK*, JANUSZ RYŚ*, JOANNA PIENIĄŻEK*, JOANNA KOWALSKA*

DEVELOPMENT OF RECRYSTALLIZATION TEXTURE IN AUSTENITIC STEEL WITH FERRITE PRECIPITATES

ROZWÓJ TEKSTURY REKRYSTALIZACJI W STALI AUSTENITYCZNEJ Z WYDZIELENIAMI FERRYTU

The object of investigations was two-phase steel having the austenitic structure with ferrite precipitates (volume fraction about 10%). The material was subjected to cold rolling up to about 85% of deformation and subsequently annealed within the temperature range 750°C÷1000°C. X-ray investigations included the phase analysis, measurements of pole figures and calculations of the orientation distribution functions (ODF's) for both component phases. The textures of austenite and ferrite after the final rolling reduction and successive stages of annealing were analysed within the centre and surface layers of the sheets. Examination of the austenite recrystallization texture included additionally the analysis of orientation fibres and transformations of the experimental and ideal ODF's.

From the texture analysis it results that the mechanisms controlling the development of the austenite recrystallization texture is the selective growth of twins. Texture simulations indicate that austenite rolling texture can be transformed into the recrystallization texture according to twin relation, i.e. by rotation through an angle of $(2n-1)\times 60°$ about <111>poles. A certain contribution of the oriented growth into the texture formation was also found. In that case relation between the recrystallization and deformation textures may be described by rotation 30°÷40°/<111>. In both cases a variant selection of the rotation axis takes place. Based on the texture examination and the phase analysis it is additionally assumed that the $(\alpha \rightarrow \gamma)$ phase transformation may exert some effect on the recrystallization textures of both component phases.

Przedmiot badań stanowiła stal dwufazowa o strukturze austenitycznej z wydzieleniami ferrytu (udział objętościowy około 10%). Materiał poddano walcowaniu na zimno do około 85% odkształcenia a następnie wyżarzano w zakresie temperatur 750°C÷1000°C. Badania rentgenowskie obejmowały analizę fazową, pomiary figur biegunowych oraz obliczenia funkcji rozkładu orientacji (FRO) dla obu składowych faz. Tekstury austenitu i ferrytu, po końcowym

* WYDZIAŁ METALURGII I INŻYNIERII MATERIAŁOWEJ, AKADEMIA GÓRNICZO-HUTNICZA, 30-059 KRAKÓW, AL. MICKIEWICZA 30

stopniu odkształcenia oraz kolejnych etapach wyżarzania, analizowano w warstwach środkowej i powierzchniowej blach. Badania tekstury rekrystalizacji austenitu obejmowały dodatkowo analizę włókien orientacji oraz transformacje eksperymentalnych oraz idealnych FRO.

Z analizy tekstury wynika, że mechanizmem kontrolującym rozwój tekstury rekrystalizacji austenitu jest selektywny wzrost bliźniaków. Symulacje tekstury wskazują, że teksturę walcowania austenitu można przekształcić w teksturę rekrystalizacji zgodnie z relacją bliźniaczą, tj. poprzez rotacje o kąt $(2n-1)\times 60°$ wokół biegunów <111>. Stwierdzono również pewien udział mechanizmu zorientowanego wzrostu w tworzeniu tekstury rekrystalizacji. W tym przypadku relację pomiędzy teksturami rekrystalizacji i odkształcenia można opisać rotacją $30°\div 40°/<111>$. W obu przypadkach ma miejsce selektywny wybór osi obrotu. W oparciu o badania tekstury oraz analizę fazową zakłada się ponadto, że pewien wpływ na tekstury rekrystalizacji obu składowych faz może wywierać przemiana fazowa $(\alpha \rightarrow \gamma)$.

1. Introduction

There are three different types of processes that give rise to the texture formation in two-phase (γ/α) steels, namely, plastic deformation, recrystallization and phase transformations. Their contribution into the texture development depend on the chemical and phase composition, conditions of plastic working and annealing treatment, initial textures and grain size of both component phases, etc. [1÷3].

Different mechanisms are involved in plastic deformation of austenitic-ferritic steels. Apart from the slip mode of deformation, mechanical twinning may proceed within the γ-phase due to relatively low stacking fault energy (SFE) of austenite [4, 5]. Additionally deformation induced $(\gamma \rightarrow \alpha)$ phase transformation may occur as a consequence of phase instability [1, 2]. As the result of twinning the {111}<uvw> orientations appear in the rolling textures of austenite but the dominant components at high strains are the {110}<uvw> orientations including the {110}<112> orientation of alloy type [2, 4].

Another aspect is the behaviour of previously deformed two-phase steels upon thermal treatment and the relation between the textures after deformation and recrystallization. Changes of deformation textures during annealing result from recrystallization processes and may be accompanied by the occurrence of the inverse $(\alpha \rightarrow \gamma)$ phase transformation [3, 6]. The formation of recrystallization textures proceeds in two stages, namely, nucleation and growth of nuclei, and is usually connected with the appearance of recrystallization twins in low-SFE γ-phase [7,8]. The concepts of continuous ("in situ") and discontinuous recrystallization, and the theories of oriented nucleation or oriented growth, including selective growth of twins, are employed to explain the development of recrystallization textures [7÷9].

The present work concerns some aspects of the formation and development of the recrystallization texture in the austenite-based two-phase steel with small volume fraction of ferrite. The steel was subjected to cold rolling up to 85% of deformation and subsequently annealed within the temperature range 750°C÷1000°C. The main purpose of the investigation was the analysis of austenite and ferrite annealing textures, within the centre and surface layers of the sheets in relation to the rolling textures of both component phases and the textures of single-phase austenitic steels [4].

2. Experimental procedure

2.1. Material

The chemical composition of the steel under examination is given in Table 1. The material in a form of ingot was homogenized and then subjected to hot working. Subsequently the rectangular bars (18×32mm) were annealed at the temperature 1050°C for 3 hours and quenched in water. Austenite and ferrite volume fractions calculated on the base of the chromium and nickel equivalents were estimated for about 90% and 10% respectively. X-ray phase analysis performed after the solution treatment confirmed the calculated volume fractions of both phases.

TABLE 1

Chemical composition of the steel (in weight %)

C	Cr	Ni	Si	Mn	Mo	V	Ti	Cu	S	P	Fe
0.07	23.91	11.09	0.30	0.20	0.009	0.074	0.019	0.058	0.023	0.010	bal.

After the preliminary treatment the steel bars were cold-rolled up to 85% of deformation (ε_t = 1.9). Reversed rolling without lubricant was applied, taking medium reductions per pass (ε = 0.02÷0.12). Following the rolling deformation the specimens were annealed at the temperatures 750, 800, 950 and 1000°C for various times ranging from 15 to 60 minutes and subsequently quenched in water.

2.2. Metallographic examination

Structure observations, based on the metallographic examination, were conducted by means of Zeiss optical microscope Neophot-2. Specimens were cut perpendicularly to the transverse direction (TD) so as to analyse the longitudinal sections (ND-RD) of the sheets. Additionally the cross sections (ND-TD) were also observed. Electrolytic etching was applied to reveal the initial structure after the solution treatment (Fig. 1a,b) and the structures after 85% of rolling reduction and subsequent annealing at the temperatures 800°C and 1000°C (Fig. 2a÷c). The morphology of ferrite after deformation and recrystallization was revealed by applying chemical etching (Fig. 3a,b).

2.3 X-ray measurements

X-ray investigations included the texture measurements (Figs. 5÷10) and the qualitative phase analysis (Fig. 14) conducted by means of Brucker diffractometer D8 Advance, using $Co_{K\alpha}$ radiation ($\lambda_{K\alpha}$ = 1.79A). Texture measurements were carried out

by means of the back-reflection method from the centre and surface layers of the sheet after 85% of rolling reduction (Fig. 5) and after annealing at temperatures 750, 800, 950 and 1000°C (Figs. 6, 7 and 10). Measurements of incomplete pole figures were recorded of three planes for each of the component phases, namely: the {111}, {100} and {110} planes for austenite and the {110}, {100} and {211} planes for ferrite. Examination of the texture development in both phases was performed by analysing the orientation distribution functions ODF's calculated from the pole figures, following the series expansion method proposed by Bunge [10]. Simulated transformations of the experimental and ideal ODF's (Figs. 11, 12 and 13) and the analysis of the orientation fibres (Figs. 8 and 9) were performed. The most important fibres are schematically presented within the three-dimensional Euler's space (φ_1, ϕ, φ_2) in figure 4.

3. Analysis of experimental results

3.1. Structure observations

The initial structures after the preliminary treatment, observed on the longitudinal and cross sections of the rectangular bars, consist in equiaxial austenite grains with clearly visible recrystallization twins (Fig. 1a,b). Small ferrite grains (precipitates) are uniformly distributed on the cross sections of the specimens, mainly on the austenite grain boundaries. The structure on the longitudinal sections exhibits slight banding of the ferrite precipitates, which are elongated parallel to the direction of hot plastic working.

The structures after 85% of rolling reduction and after annealing at the temperature 800°C for 1 hour show high degree of banding, with thin and continuous ferrite bands elongated parallel to the rolling plane (Fig. 2a,b). The structural effects of plastic deformation, remaining in the form of strongly banded structure with characteristic

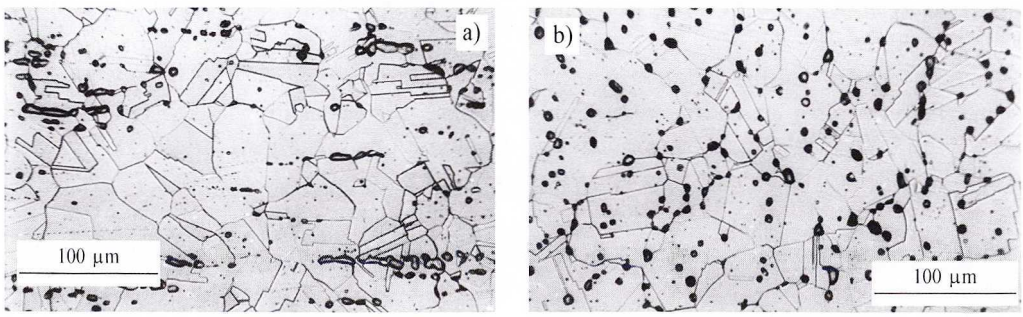

Fig. 1. Initial structure after the solution treatment showing the distribution of ferrite precipitates against the austenite background on the longitudinal section ND-RD (a) and the cross section ND-TD (b) of the specimen; electrolytic etching

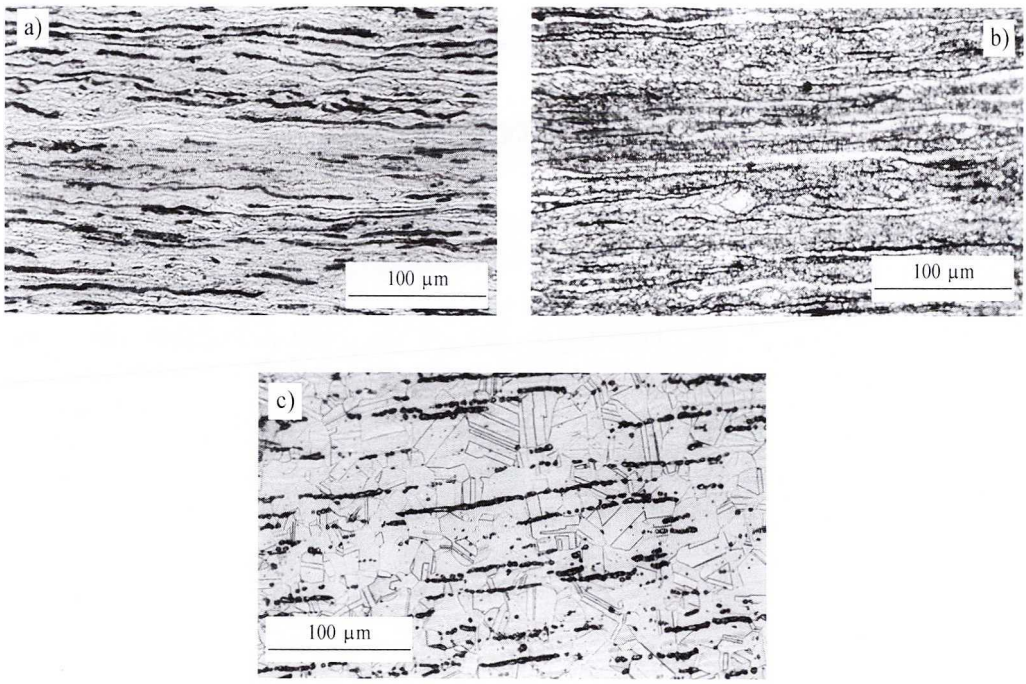

Fig. 2. Structures of the steel after 85% of deformation (a), annealing at 800°C/1h (b) and recrystallization at 1000°C/1h (c) on the longitudinal section ND-RD of the sheet; electrolytic etching.

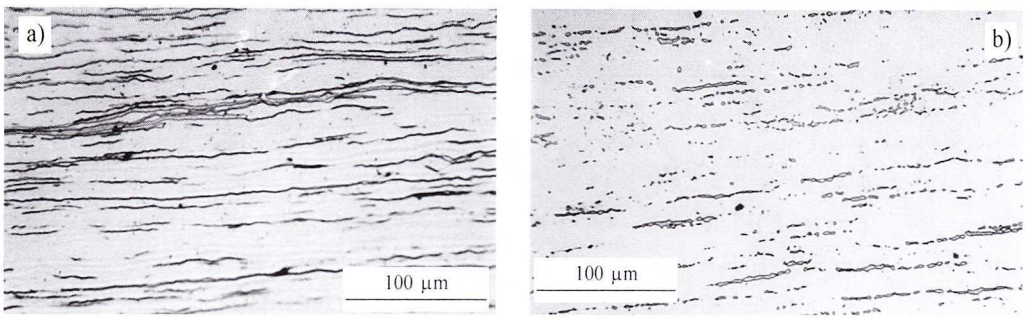

Fig. 3. Two-phase structure revealed by chemical etching showing the morphology of ferrite after 85% of deformation (a) and recrystallization at 1000°C/1h (b); (longitudinal section ND-RD)

rhomboidal blocks within the austenite matrix, indicate that the material subjected to annealing at 800°C/1h is not entirely recrystallized (Fig. 2b).

Complete primary recrystallization of the steel cold-rolled up to 85% of reduction occurred after annealing at the temperature 1000°C (Fig. 2c). Within the recrystallized

structure the austenite grains and the recrystallization twins are visible, which are markedly smaller in comparison to those in the initial material.

A change in the morphology of the ferrite precipitates is also observed. Instead of thin and continuous bands, ferrite is present in the form of fine precipitates arranged parallel to the rolling direction (Fig. 3a,b).

3.2. Rolling textures

Characteristic orientation fibres (Fig.4) describe the orientation distribution in the austenite rolling texture after 85% of reduction. In the α-fibre (<110>||ND), which extends from {011}<100> to {011}<111>, the strongest texture components are the {011}<311> and {011}<511> orientations within the surface and centre layers of the sheet respectively (Figs. 5, 8 and 9). Another fibres, which describe the austenite deformation texture, are the limited τ-fibre (<110>||TD) as well as weak γ-fibre (<111>||ND).

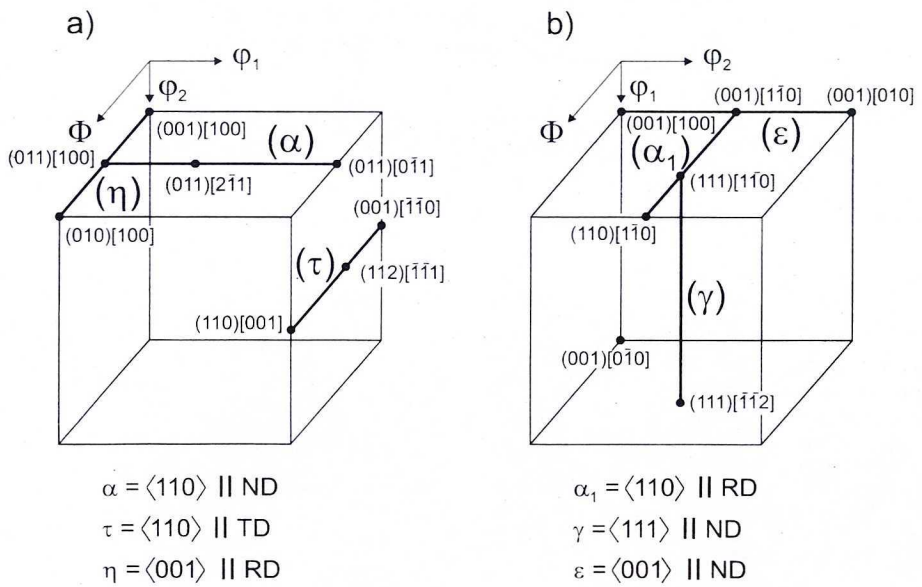

Fig. 4. Schematic representation of the most important fibres and orientations within the three-dimensional Euler's space for the case of fcc (a) and bcc (b) phases

The texture of ferrite after deformation is relatively weak and spread with the α_1-fibre (<110>||RD) and the {332}<113> orientations apparent in the rolling texture of both layers (Fig.5). The strongest component of the ferrite texture in the surface layer is the {449}<110> orientation (close to the {112}<110>). It belongs to the α_1-fibre, which

extends from {001} to {111}. In the ferrite texture of the centre layer the α_1-fibre is weak and the orientation density along that fibre is nearly constant.

Similarly to the austenite matrix, the ferrite precipitates are plastically deformed upon rolling, hence their presence in the structure should not introduce any qualitative changes in the austenite rolling texture [11]. On the other hand, the occurrence of deformation induced ($\gamma \rightarrow \alpha$) phase transformation, which is assumed to result from the phase instability, may be the reason of some changes in the rolling textures of both

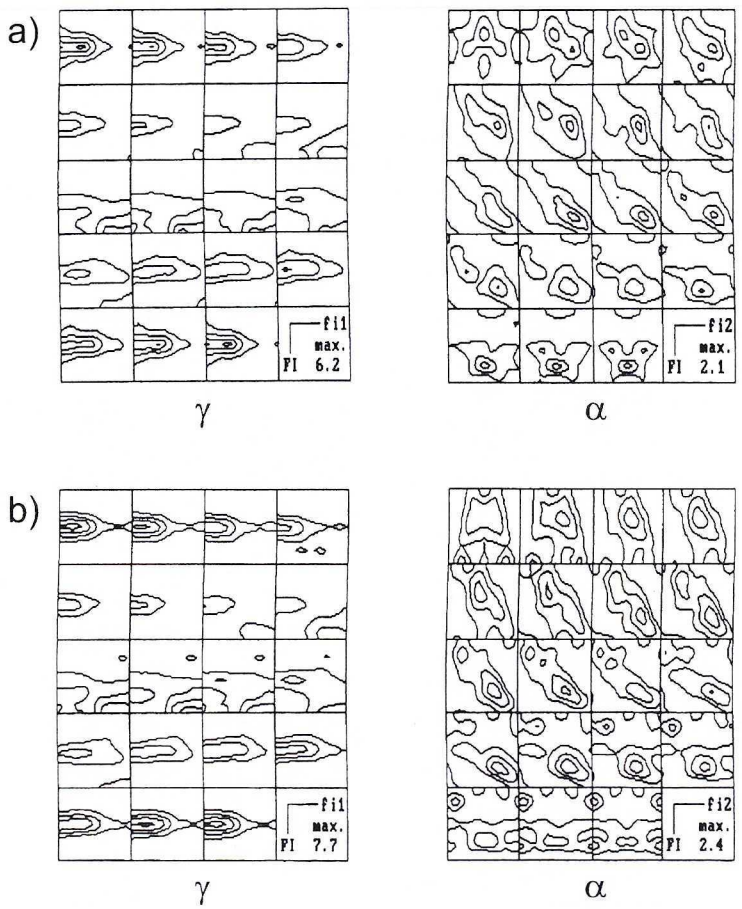

Fig. 5. Orientation distribution functions in sections φ_2 = const for the γ-phase and φ_1 = const for the α-phase after 85% of deformation from the surface (a) and the centre (b) layer of the rolled sheet

phases [1, 2]. Crystallographic relations between the major components of the austenite and ferrite rolling textures under examination are well described by **K-S** orientation relationship.

3.3. Austenite annealing textures

The first stages of annealing lead to the significant spread of the austenite rolling texture within the surface and centre layers of the sheet (Fig. 6). An extension of the α-fibre from {011}<100> to {011}<011> is observed in the austenite texture after annealing at the temperature 750°C for 30 and 60 minutes. The α-fibre is relatively weak with nearly constant orientation density. Intensity of the {011}<100> component was considerably weakened. On the other hand, the {011}<211> and {011}<011> orientations are distinguishable however still weak. The strongest texture component is the {113}<332> orientation from the τ-fibre (Table 2). Moreover, the η-fibre appeared

TABLE 2

Maximum values of the ODF's and the corresponding ideal orientations in the austenite texture of the centre and surface layers

Annealing temperature	Annealing time	Centre layer		Surface layer	
		Orientation	ODF max.	Orientation	ODF max.
85 % def.	—	(011) [$5\bar{1}1$]	7.5	(011) [$3\bar{1}1$]	6.1
750°C	30 min	(113) [$33\bar{2}$]	1.9	(113) [$33\bar{2}$]	2.0
750°C	60 min	(113) [$33\bar{2}$]	1.9	(113) [$33\bar{2}$]	1.9
800°C	30 min	(113) [$33\bar{2}$]	1.7	(113) [$33\bar{2}$]	1.9
800°C	60 min	(113) [$33\bar{2}$]	1.7	(113) [$33\bar{2}$]	2.0
950°C	15 min	(113) [$33\bar{2}$]	2.0	(113) [$33\bar{2}$]	2.7
950°C	30 min	(113) [$33\bar{2}$]	2.3	(034) [$0\bar{4}3$]	2.3
950°C	60 min	(113) [$33\bar{2}$]	2.0	(034) [$0\bar{4}3$]	2.3
1000°C	20 min	(034) [$0\bar{4}3$]	2.8	(011) [$0\bar{1}1$]	3.0
1000°C	30 min	(034) [$0\bar{4}3$]	3.2	(011) [$0\bar{1}1$]	3.2
1000°C	60 min	(034) [$0\bar{4}3$]	2.8	(011) [$0\bar{1}1$]	2.8

in the austenite texture and extends from the {100}<001> cubic orientation to the {011}<100> Goss orientation, whereas the γ-fibre (<111>||ND) completely disappeared.

The texture of austenite annealed at higher temperatures exhibits similar character (Figs. 6 and 7). At 800 and 950°C a spread along the α-fibre is still remaining with the

maximum orientation density shifted toward the {011}<011> orientation. Maximum values of the ODF's correspond to the {113}<332> orientation within the centre layer and the {034}<043> orientation (~ 12° from the {011}<011>) at the surface (Table 2). After annealing at the temperature 1000°C the orientation distribution does not change essentially (Fig. 7). The following orientation fibres describe the austenite texture, namely, the α-, τ- and η-fibres (Figs. 8 and 9). The α-fibre (<011>||ND) is spread and extends from {011}<100> to {011}<011>. The strongest texture components are the {034}<043> orientation within the centre layer of the sheet and the {011}<011> orientation at the surface (Table 2). The {113}<332> orientation remains distinguishable texture component of austenite after annealing.

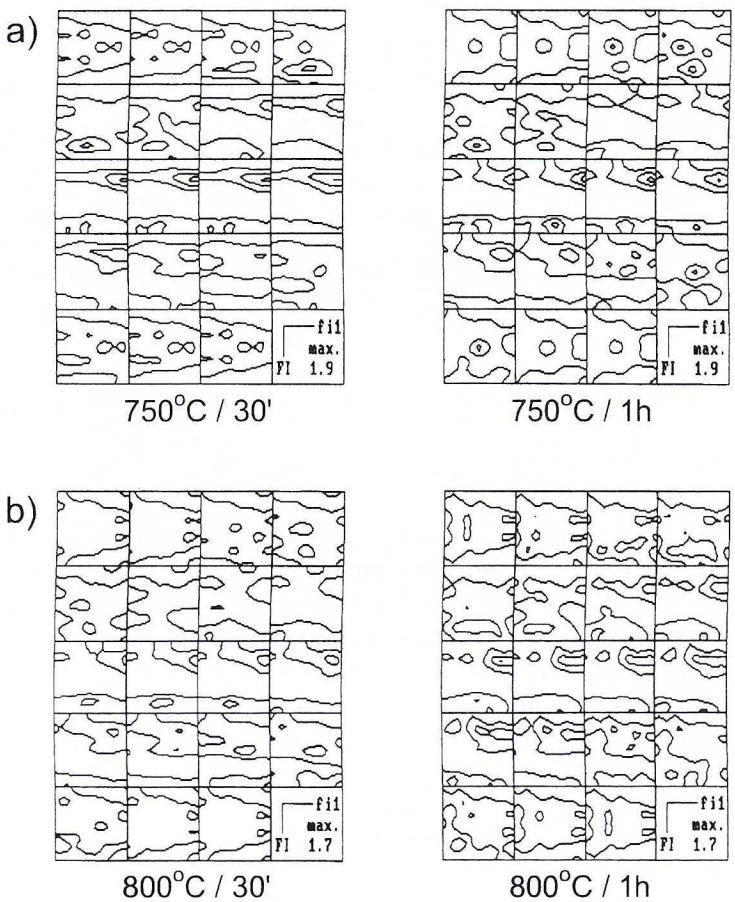

Fig. 6. Orientation distribution functions in sections φ_2 = const for the γ-phase after annealing at the temperatures 750°C (a) and 800°C (b) for 30 and 60 min; centre layer

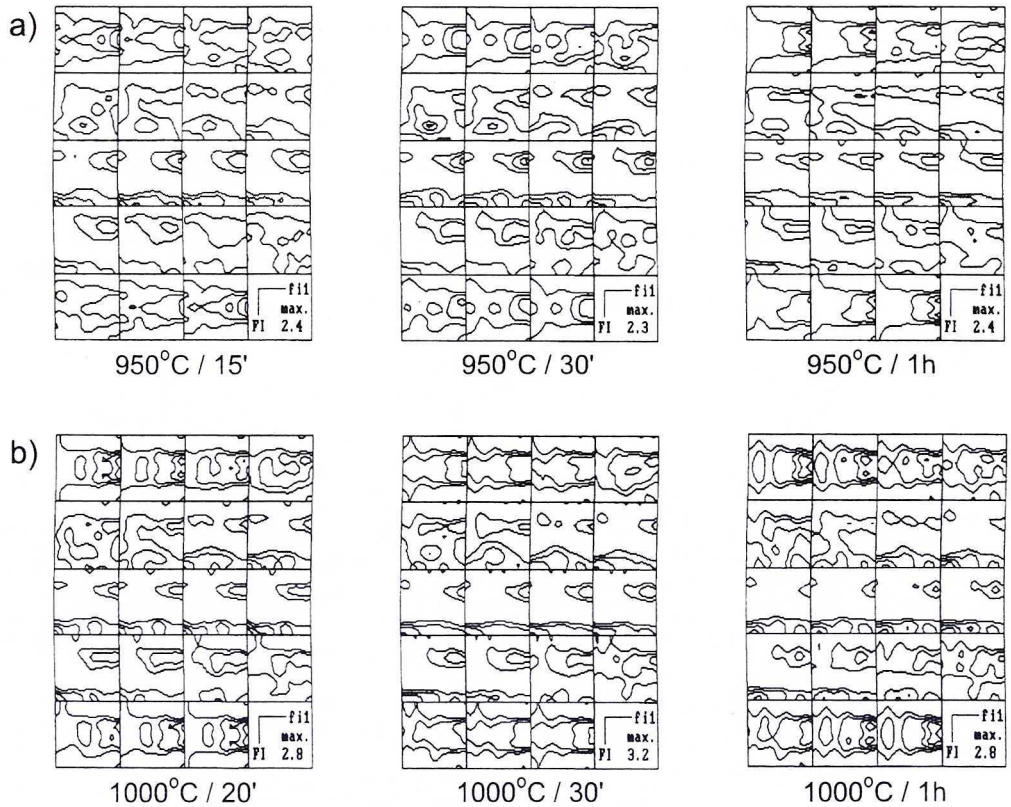

Fig. 7. Orientation distribution functions in sections φ_2 = const for the γ-phase after annealing at the temperatures 950°C for 15, 30 and 60 min (a) and 1000°C for 20, 30 and 60 min (b); centre layer

In general, the examination of the texture development indicates, that differences in the austenite recrystallization texture between the surface and centre layers of the sheet are insignificant (Figs. 8 and 9, Table 2). Thus the major changes of the austenite texture observed during annealing for both layers may be described as follows:

- spread of the austenite texture and extension of the α-fibre (<011>$\|$ND) at early stages of annealing;
- displacement of the maximum intensity within the α-fibre toward the {011}<011> orientation component;
- decay of the weak γ-fibre (<111>$\|$ND);
- appearance of the new orientations within the τ-fibre (<110>$\|$TD), namely the {113}<332> orientation;
- formation of new texture components ~{034}<043>;
- appearance of the {326}<835> orientation, which is the characteristic texture component for the low-SFE materials.

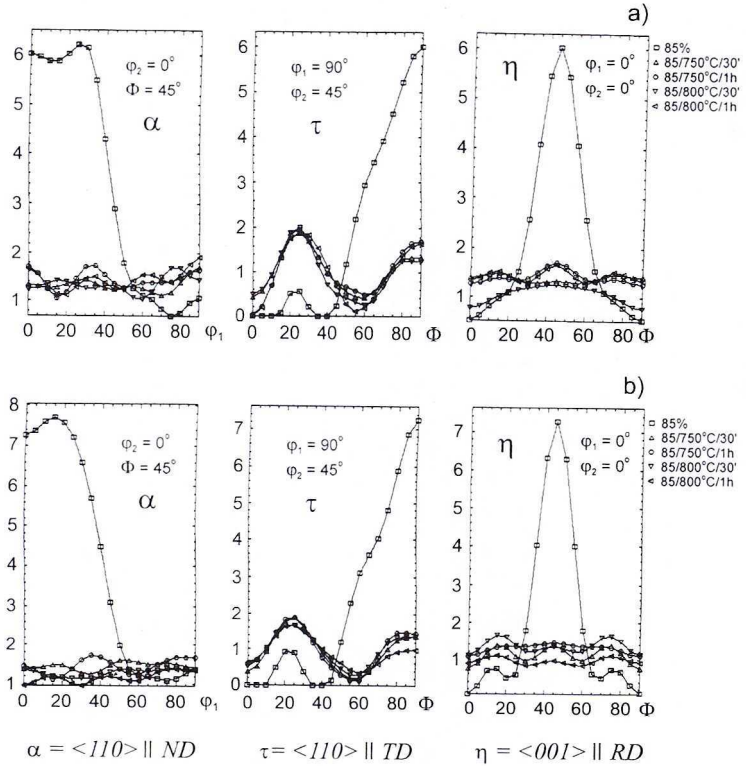

Fig. 8. Values of the orientation distribution function f (g) for the γ-phase along the α-, τ- and η-fibres in specimens after 85% of deformation and annealing at 750°C and 800°C; surface and centre layer (a and b — respectively)

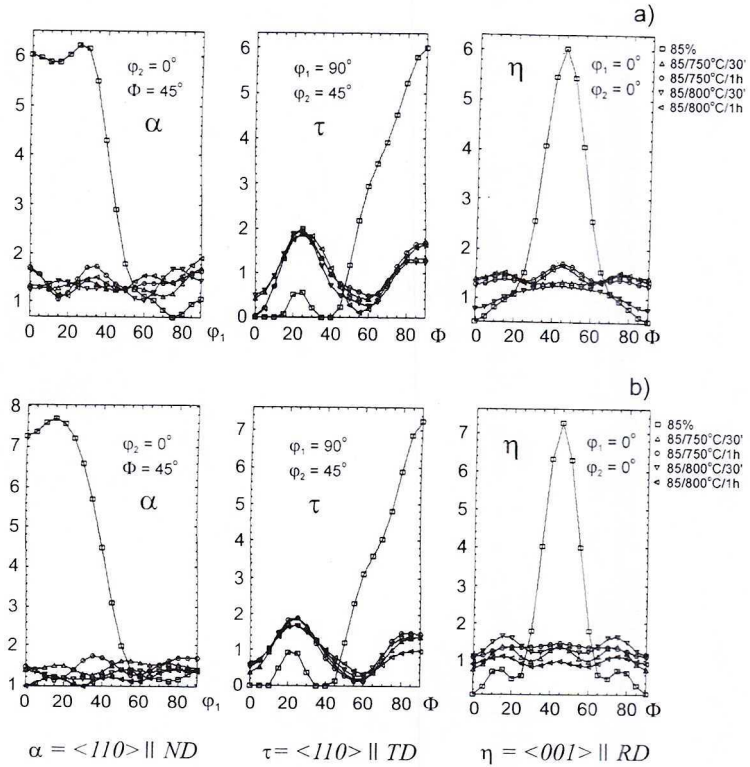

Fig. 9. Values of the orientation distribution function f (g) for the γ-phase along the α-, τ- and η-fibres in specimens after 85% of deformation and annealing at 950°C and 1000°C; surface and centre layer (a and b — respectively)

3.4. Ferrite annealing textures

A considerable spread of the ferrite texture is observed after annealing at the temperatures 750°C and 800°C for 30 and 60 minutes (Fig. 10a). It resulted in a weakening (surface layer) or decay (centre layer) of the intensity of the major components of the ferrite deformation texture, i.e. the orientations from the α_1-fibre (<110>||RD). Only single orientations are distinguishable against the background of the very weak annealing texture of ferrite, for example the {772}<uvw> and ~{010}<100> orientations from the centre and surface layers respectively.

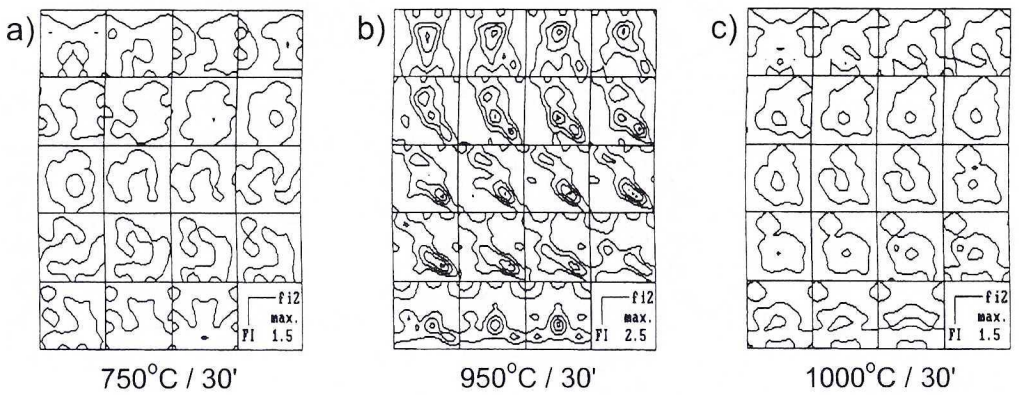

Fig. 10. Orientation distribution functions in sections φ_1 = const for the α-phase after annealing at the temperatures 750°C (a), 950°C (b) and 1000°C (c); centre layer

Annealing at the temperature 950°C for 30 minutes gives rise to relatively higher intensity of the ferrite texture, which in part exhibits fibrous character (Fig. 10b). The limited α_1-fibre is essentially preserved within the texture of the centre layer. Orientations close to the {113}<110> and {112}<110> are relatively strong texture components, however their intensities diminished when the annealing time was prolonged up to 60 minutes. Additionally the homogenous γ-fibre (<111>||ND) is observed, which is very weak and spread, with the strongest components {111}<110> and {111}<112> as well as the orientations of {332}<uvw> type within the texture of the centre layer. On the other hand the strongest component in the surface layer is the (111)[$\bar{1}\,\bar{3}$4] orientation close to the (111)[0$\bar{1}$1].

Increase of the temperature up to 1000°C and annealing for 30 minutes resulted again in significant decrease of the texture intensity (Fig. 10c). Against the background of very weak or nearly random texture single orientations from the (α_1-fibre {113÷332}<110> are distinguishable and the orientations such as (015)[0$\bar{5}$1].

4. Discussion

4.1. Texture transformations upon recrystallization

For a given specific orientation relationship there exists an axis, which is invariant with respect to the transformation. Hence the crystallographic relation may be described as a rotation of an angle about the common axis [1, 7]. According to the theory of oriented growth one of the most important factors controlling the development of recrystallization textures is the orientation dependence of grain growth rate. It assumes that nuclei of all crystallographic orientations are present at the onset of recrystallization and the resulting recrystallization texture depends on which orientations are growing faster into the deformed matrix. For the case of face centred cubic (FCC) materials the growth rate is a maximum when the orientation relationship between the deformed material and the growing grain is described by rotation of about 40° around the <111> axis [7÷9]. Similarly, for the case of selective growth of primary or secondary recrystallization twins the crystallographic relation between the matrix and the growing twin may be characterized by rotation of 60° (or 180°) about the <111> axis [7÷9]. It means, that in the case of low-SFE materials the deformation texture may be transformed into the recrystallization texture by $\sim 40°/<111>$ or $(2n-1)\times 60°/<111>$ rotations. To estimate a contribution of both mechanisms into the development of the austenite recrystallization texture in the steel under examination, transformations of the ODF's calculated from the pole figures as well as transformations of the selected ideal orientations were performed according to above relations.

4.2. Development of austenite recrystallization texture

Figures 11c and 11d present the transformed ODF's obtained from the austenite deformation texture (Fig.11a) by rotations 40° and 180° respectively about the <111> common poles. Analysis of the transformed ODF's and the austenite texture after annealing at 1000°C/30′ (Fig.11b) indicates that crystallographic relations between orientations, which are present in the austenite deformation texture and the orientations from the recrystallization texture are well described by twin relationship, i.e. rotations through an angle of $(2n-1)\times 60°$ about the <111> common poles. There are however some orientation relations, resulting from rotations of about 40° around <111> axes, which are connected with the mechanism corresponding to the theory of oriented growth. In the case of both mechanisms a variant selection takes place, which is connected with the selective choice of the rotation axis, since not all possible transformations are accomplished during the process of recrystallization.

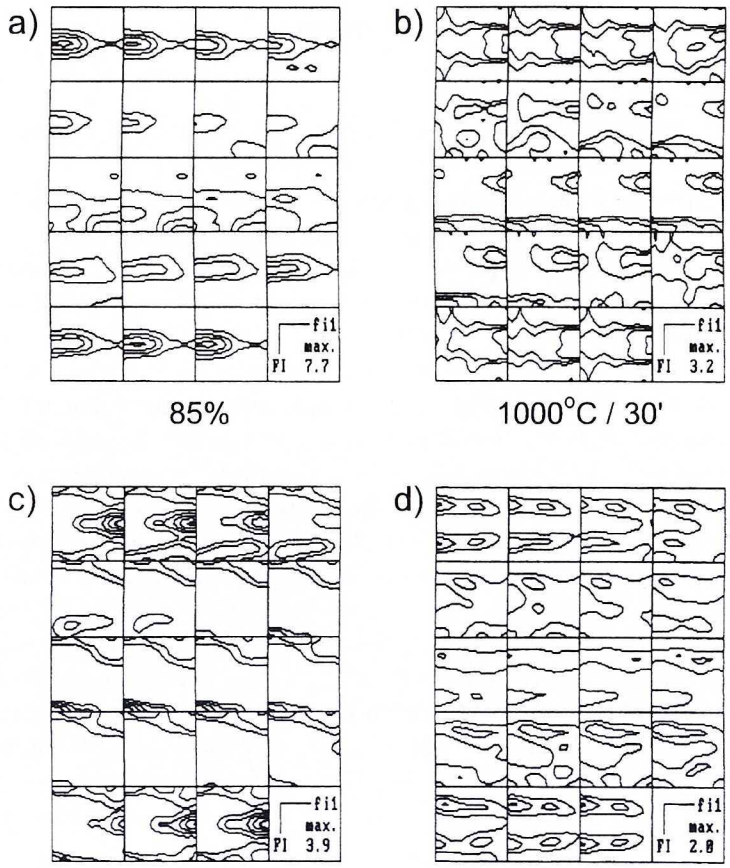

Fig. 11. Experimental ODF's of the γ-phase after 85% of deformation (a) and recrystalization at 1000°C (b), and simulated ODF's transformed according to 40°<111> and 180° <111> rotations (c and d respectively)

Comparison of the transformed and experimental ODF's after recrystallization (Fig.11) indicates at the selective choice of the rotation axes. It means that new orientations appear in the course of annealing due to the selective growth of nuclei with certain preferential orientations. It occurs that the mechanism controlling the formation of austenite recrystallization texture is the selective growth of twins. It is additionally confirmed when analysing the ideal {110}<uvw> orientations from the rolling texture and the orientations of {113}<uvw> type from the recrystallization texture transformed according to twin relation (Fig. 12). A certain contribution of the oriented growth into the texture formation was also found. In that case relation between the recrystallization and deformation textures may be described by rotations 30°÷40°/<111>. Figure 13 presents the ideal orientations from the austenite recrystallization texture transformed according to 32°/<111>, 42°/<111> and 60°/<111> rotations, namely, the (034)[0$\bar{4}$3] orientation, which is the strongest component of the annealing texture, and the (326)[83$\bar{5}$], which is a typical alloy type orientation of the recrystallization texture.

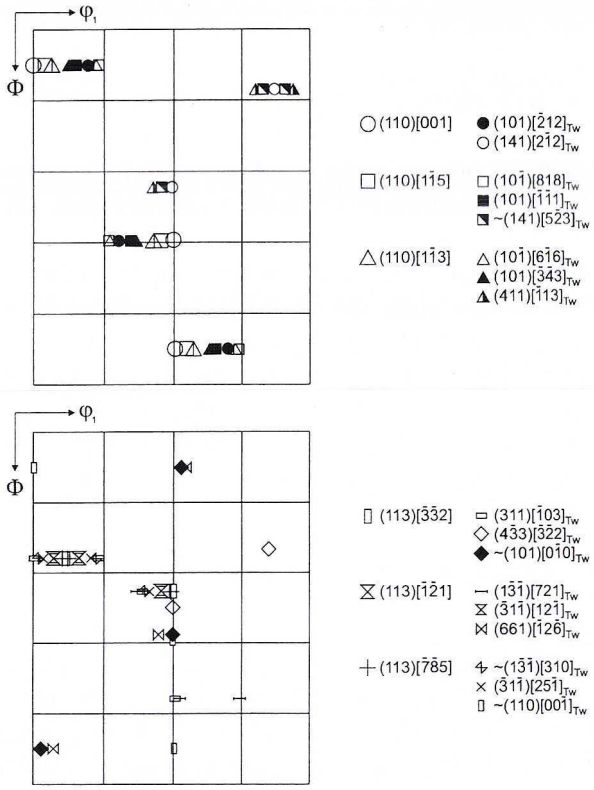

Fig. 12. Transformatins of the ideal {110}<uvw> orientations (α-fibre) from the rolling texture and the {113}<uvw> orientations from the recrystallization texture according to twin relation (section φ_2 = const)

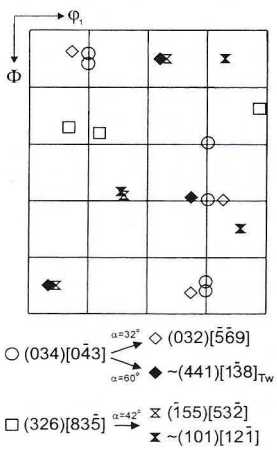

Fig. 13. Transformations of the ideal orientations (034)[$0\bar{4}3$] and (326)[$83\bar{5}$] from the austenite recrystallization texture according to 32°<111>, 60°<111> and 42°<111> rotations (section φ_2 = const)

The texture analysis indicates at the weakening or decay of some texture components from the austenite deformation texture and the appearance of new orientations during recrystallization annealing. Contrary to the results obtained by D o n a d i l l e et. al. [4], there is no retainment of the major texture components although the -fibre was found both in the rolling and annealing textures of austenite. The present results seem to indicate unambiguously at a discontinuous character of the recrystallization process. Appreciable spread of the austenite rolling texture (nearly random orientation distribution) at lower annealing temperatures (Fig.6) may be explained by the appearance of many nuclei of all orientations at the very beginning of recrystallization. Different annealing behaviour of cold-rolled austenite in the case of steel examined by D o n a d i l l e et. al. [4] is attributed to a strong solute effect of molybdenum addition, which reduces dislocation mobility and hence affects nucleation processes.

4.3. Changes of ferrite texture upon annealing

Results of the phase analysis (Fig. 14) and changes of the intensity of the ferrite texture (Fig. 10 a÷c) after the successive stages of annealing seem to indicate at a certain effect of the σ-phase precipitation on the ferrite annealing texture within the lower range of annealing temperatures. A considerable spread and weakening of the ferrite texture at the temperatures 750°C and 800°C may result from both, the precipitation of the σ-phase and its effect on nucleation processes [11,12]. The major components of the ferrite texture have the highest intensities upon annealing at the temperature 950°C, i.e. after dissolution of the σ-phase, with the limited (α_1-fibre essentially preserved within the annealing texture. On the other hand considerable spread and weakening of the ferrite texture, revealed once again upon annealing at the higher temperatures, suggest the occurrence of the ($\alpha \rightarrow \gamma$) phase transformation. Diffraction patterns recorded after

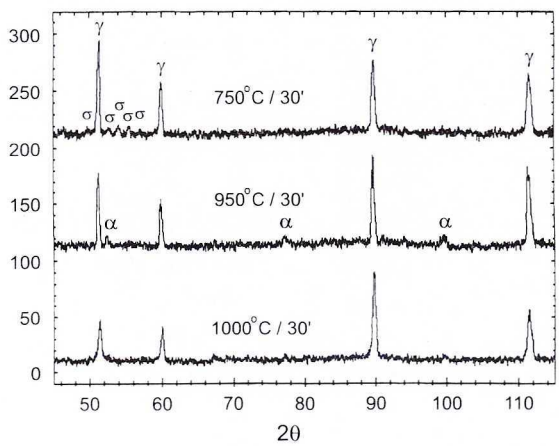

Fig. 14. X-ray diffraction patterns of specimens after annealing at 750°C, 950°C and 1000°C from the centre layers of the rolled sheets

annealing at 1000°C confirm significant decrease or even complete decay of reflections coming from the α-phase (Fig. 14). In such case it is assumed that the ($\alpha \rightarrow \gamma$) phase transformation may exert some effect on the development of the austenite recrystallization texture [3,6]. In some part the orientation relations between recrystallization textures of both phases are described by K–S relationship.

5. Conclusions

1. Appreciable spread of the austenite rolling texture (nearly random orientation distribution) in early stages of annealing may be explained by the appearance of many nuclei of all orientations at the very beginning of recrystallization.

2. Significant weakening or decay of some texture components from the austenite deformation texture and the appearance of new components in the course of recrystallization annealing indicates at selective growth of nuclei.

3. Both the spread of the austenite deformation texture upon annealing and the appearance of new orientations in the austenite recrystallization texture confirm a discontinuous character of the recrystallization process.

4. Analysis of the experimental and transformed ODF's indicates that recrystallization proceeded by means of nucleation and selective growth of twins with a certain contribution of the mechanism of oriented growth.

5. From texture transformations it results that the deformation texture of austenite may be transformed into the recrystallization texture by rotations of $(2n-1)\times 60°$ angles around the <111> poles and to some extend by $30°\div 40°/<111>$ rotations, with regard to the selective choice of the rotation axis in both cases.

6. Based on the texture examination and the phase analysis it is assumed that, the σ-phase precipitation and the ($\alpha \rightarrow \gamma$) phase transformation may exert some effect on the textures of the component phases within the lower and higher range of annealing temperatures respectively.

Acknowledgements

The authors gratefully acknowledge financial support from the Polish Committee of Scientific Research (KBN) under the contract No 11. 110.230.

REFERENCES

[1] R.K. Ray, J.J. Jonas, Transformation textures in steels, International Materials Reviews **35**, 1 (1990).
[2] W. Ratuszek, J. Ryś, K. Chruściel, Effect of deformation mode on texture development in cold-rolled duplex steel, Archives of Metallurgy **44**, 305 (1999).
[3] W. Ratuszek, J. Ryś, M. Karnat, Annealing textures in cold-rolled duplex type steel, Archives of Metallurgy **45**, 57 (2000).

[4] C. Donadille, R. Valle, P. Dervin, R. Penelle, Development of texture and microstructure during cold-rolling and annealing of fcc alloys: example of an austenitic stainless steel, Acta Metallurgica **37**, 1547 (1989).
[5] M. Blicharski, Rekrystalizacja stali austenitycznych chromowo-niklowych, Hutnik, **44**, 129 (1977).
[6] G. Bruckner, J. Pospiech, Modelling and verification of texture development during the ($\alpha \rightarrow \gamma$) phase transformation in steel, Proc. 11-th Int. Conf. on Textures of Materials, ICOTOM-11, China, 598 (1996).
[7] K. Lücke, The formation of recrystallization textures in metals and alloys, Proc. 7-th Int. Conf. on Textures of Materials, ICOTOM-7, Nordvijkerhout, 195 (1984).
[8] A. Berger, P.-J. Wilbrandt, F. Ernst, U. Klement, P. Haasen, On the generation of new orientations during recrystallization, Progress in Materials Science **32**, 1 (1988).
[9] W. Ratuszek, Tekstury odkształcenia i rekrystalizacji w stopach na osnowie miedzi, Rozprawy i monografie, Wyd. AGH, Kraków, (1995).
[10] H.J. Bunge, Texture Analysis in Materials Sciences, Butterworths, London 1982.
[11] K. Lücke, O. Engler, Effects of particles on development of microstructure and texture during rolling and recrystallization in fcc alloys, Materials Science and Technology **6**, 1113 (1990).
[12] M. Blicharski, S. Gorczyca, Rekrystalizacja z udziałem drugiej fazy, Wyd. Śląsk, Katowice (1980).

REVIEWED BY: JERZY JURA
Received: 12 April 2002.